THERMAL REDUCTION OF Cu^{2+} IN PRESENCE OF Ag^{+} IN CLINOPTILOLITE: STRUCTURAL STUDY BY EXAFS AND HR-XRD

REDUCCIÓN TÉRMICA DE Cu^{2+} EN PRESENCIA DE Ag^{+} EN CLINOPTILOLITA: ESTUDIO ESTRUCTURAL POR EXAFS Y HR-XRD

B. Concepción-Rosabal[a†], I. Rodríguez-Iznaga[b] ,V. Petranovskii[c], F. Chávez Rivas[d], S. J. A. Figueroa[e], A. Pentón-Madrigal[b]

a) Instituto de Ciencia y Tecnología de Materiales (IMRE) - Universidad de La Habana, Cuba; beatriz@imre.uh.cu†
b) Facultad de Física- IMRE, Universidad de La Habana, La Habana, Cuba
c) Centro de Nanociencias y Nanotecnología (CNyN) – Universidad Nacional Autónoma de México. Carretera Tijuana-Ensenada, Km 107. Ensenada, B.C. México
d) Escuela Superior de Física y Matemáticas, Instituto Politécnico Nacional (IPN), C.P. 07738, México, D.F., México
e) Brazilian Synchrotron Light Laboratory (LNLS)/Brazilian Center of Energy and Materials (CNPEM), CP 6192, 13083-970, Campinas, SP, Brazil
† corresponding author

Recibido 14/5/2019; Aceptado 12/11/2019

Cu^{2+}–Ag^{+} bimetallic systems were exchanged and then thermally reduced in natural clinoptilolite (CLI) from Tasajeras deposit (Cuba). The systems were characterized by means of extended X-ray absorption fine structure (EXAFS) and high resolution X-ray diffraction (HR-XRD) experiments. The EXAFS signals of the bimetallic systems showed changes in the Cu^{2+} coordination as a result of their reduction at 150°C, which doesn't happen to CuCLI monometallic one. The presence of silver facilitates the reduction of Cu^{2+} in bimetallic systems forming only clusters. At higher reduction temperature (450°C) all mono- and bi-metallic samples exhibit mainly metallic particles of Cu and Ag with higher aggregation. These results are confirmed by HR-XRD studies. Aggregation of reduced copper species is restricted in the presence of silver.

Sistemas bimetálicos de Cu^{2+}–Ag^{+} fueron intercambiados y seguidamente reducidos térmicamente en la clinoptilolita natural (CLI) del yacimiento de Tasajeras (Cuba). Estos sistemas fueron caracterizados a través de experimentos de estructura fina de la absorción de rayos X en la región extendida (EXAFS, acrónimo en inglés) y difracción de rayos – X de alta resolución (HR-XRD, acrónimo en inglés). Las señales de EXAFS de los sistemas bimetálicos mostraron cambios en la coordinación del Cu^{2+} como resultado de su reducción a 150°C, lo cual no sucede en el sistema monometálico de CuCLI. La presencia de la plata facilita la reducción del Cu^{2+} en los sistemas bimetálicos, formándose solamente clústeres a esta temperatura. A mayor temperatura de reducción (450°C) todas las muestras mono- y bi-metálicas exhiben principalmente partículas de Cu y Ag metálico con mayor agregación. Estos resultados se confirman por estudios de HR-XRD. La agregación de las especies de cobre reducidas es restringida en presencia de la plata.

PACS: Zeolites, clusters in zeolites, structural properties, (zeolitas, clústeres en zeolitas, propiedades estructurales) 82.75.z, 82.75.Mj, 82.75.Vx; X-ray absorption spectroscopy (EXAFS) (espectroscopia de absorción de rayos X), 61.05.cj; X-ray diffraction (XRD) (difracción de rayos X), 61.05.cp

I. INTRODUCTION

Modified zeolites with metal nanospecies (ions, clusters, nanoparticles, etc.) are of interest due to their unique and improved properties to develop new materials as catalyts, drugs, bactericides and others [1–9]. Among other metals, Cu and Ag are outstanding due to both catalytic properties and olygodynamic activity. Thus, it is well-known that zeolites modified with copper cations are among the most selective and active catalysts to nitrogen monoxide (NO) reduction [1, 10–13]. It is also recognized that the type of supported metallic nanospecies, their aggregation and stability define the properties and use of modified zeolites.

Numerous studies on zeolites modified with only one metal are available in the literature. The properties of the metal species experience important changes in multimetallic systems with respect to monometallic one [1, 14–17]. In this sense, it was shown that both stability and catalytic activity in NO-reduction to Cu^{2+} catalysts supported on mordenite increase when silver is present [1]. It has been reported that Zn^{2+} has a positive effect to Cu^{2+} reduction on clinoptilolite zeolite [15].

Early structural studies [14] on thermal reduced bimetallic Cu^{2+}–Ag^{+} systems exchanged in clinoptilolite from the Tasajeras deposit (Cuba) were performed by means of UV-Vis reflectance diffuse spectroscopy and conventional X – ray diffraction. The obtained results showed a significant inter influence of both metals during the reduction process and formation of different reduced species, which was associated with a synergetic effect of the different concurrent species. UV-Vis spectra showed evidences on exchanged Cu2+ through the characteristic band of this cation associated with d-orbital transitions. A band of charge-transfer complex due to the interaction of this cation with oxygen both of ligand water molecules and of zeolite framework was observed as well, which in turn lead to the formation of

$Cu(_2^+)$-δ/CLI($_2$−)+δ and $Ag(^+)$-δ/CLI(−)+δ complexes. Besides this, it was revealed the occurrence of both copper and silver particles possessing plasma resonance absorbance at higher temperature (450oC), which is in line with reported X – ray diffraction results [4, 5]. Also, X – ray diffraction has shown peak intensities changes fundamentally associated with differences in nature, amount and position of the extra-framework ions in zeolite channels [4, 5, 18].

This work presents a study concerning the thermal reduction under hydrogen flow of a bimetallic Cu^{2+}–Ag^+ system exchanged on natural clinoptilolite from Tasajeras deposit, Cuba. The influence of silver on Cu2+ reduction was studied by means of High Resolution X – Ray Diffraction (HR-XRD) and Extended X-ray absorption fine structure (EXAFS).

II. EXPERIMENTAL

The purified zeolite material, with a particle size of 40 – 90 μm, was obtained from the zeolitic rock of Tasajeras deposit (Cuba). It is a mixture of about 78 % clinoptilolite-heulandite, 5 % mordenite and 17 % of others phases (montmorillonite, quartz, feldspar and iron oxides). The elemental chemical composition of the purified zeolite material was reported previously in [14]. Herein this zeolite is referred as the purified zeolite or natural clinoptilolite (CLI).

Copper/Silver-CLI bimetallic systems were prepared by Cu^{2+} and Ag^+ simultaneous ion-exchange using 0.1 mol/L $Cu(NO_3)_2/AgNO_3$ mixed solutions with different Cu/Ag ratios (see Table 1) and 1g/4mL liquid/solid ratio, at room temperature. After this, they were reduced at two different temperatures, 150°C and 450°C, in a hydrogen flow. The CuCLI monometallic system was also obtained in similar mode, but using 0.1mol/L $Cu(NO_3)_2$ solution, and reduced under same conditions to provide a reference from which the effects of silver addition could be investigated. The number after the sample name indicates the reduction temperature.

Table 1. Copper and silver content for exchanged zeolites samples. The number in the bimetallic samples indicates the used Cu−Ag ratio.

Samples	CuCLI	$AgCu_3CLI$	$AgCu_9CLI$
Cu (wt %)	3.40	1.44	1.50
Ag (wt %)	-	3.80	2.23

X - ray absorption spectroscopy experiments at Cu−K and Ag−K absorption edges were performed in transmission mode and at room temperature in the XAFS2 beamline of the LNLS, Campinas, Brazil [19]. The monochromator was calibrated with metallic foils placed between the second and third ionization chamber for each measured absorption edge. Samples of CuO and $AgNO_3$ were used as references. For each sample the energy scans were conducted three times for statistic improvement. Durapore Membrane Filters with 0.2 μm pore size were used to deposit the powders. The EXAFS analysis was performed using the Iffefit software package [20].

HR-XRD experiments were conducted in transmission mode at MCX beamline ELETTRA using energy of 12.399 keV and collected at room temperature. The samples were disposed in borosilicate glass capillaries (0.5 mm diameter), data were collected by means of a Pilatus detector, with fixed measuring time of 150 s, using a double crystal monochromator of Si (111).

III. RESULTS AND DISCUSSION

III.1. EXAFS EXPERIMENTS

Figure 1a shows the average $\chi(k)\cdot k^2$ signal calculated from the absorption spectra of the studied samples. The EXAFS signals of the CuCLI and $CuCLI_15_0$ samples show the same period and amplitude, this is an evidence of no changes in the local environment in this thermal treatment. The signal period is associated with Cu distances to its nearest neighbors, as shorter the period longer distances are expected. As commented for figure 1a, the reduction at 150°C does not affect the Cu coordination related to the as obtained sample (CuCLI). On the other hand, when the sample is reduced at 450°C the period of the EXAFS signal is reduced and matches the one of metallic Cu, but the signal exhibits lower amplitude. This result could be interpreted by the occurrence of Cu nanoparticles, by the important contribution that copper atoms in surface done when are in form of nanosized clusters. The EXAFS equation has a term that is direct related with the coordination number (N), if for any reason this number decreases (i.e. for metallic copper in bulk form: $N = 12$ copper for first nearest neighbors) the amplitude of the signal decreases consequently. If we assume that copper are segregate from the zeolite, this atoms could aggregate to form a nanoparticle that has an important amount of free surface. The copper atoms in the surface of this nanoparticles has a lower amount of first nearest neighbors, for this reason the average coordination number (that is the one obtained in the EXAFS fit) will decrease, given a reduction in the amplitude. Temperature effects (disorder) that can also affect the EXAFS amplitude can be consider in this case, but their effects are lower for nanoparticles bigger than 1 nm [21] , that are our case as we will show in the following. This Cu nanoparticles produced by the thermal treatment should be outside the zeolites channels.

The figure 1b shows a different behavior for the $AgCu_3CLI$ sample. In this case the amplitude and the period of the EXAFS signal of the reduced sample at 150°C ($AgCu_3CLI_15_0$) are quite different to the unreduced one, in particular for large k (wavenumber) values. These changes in amplitude and period should result as a variation in the coordination number of Cu^{2+} or as a contribution of metallic Cu emerging clusters. This result suggests that the addition of Ag^+ may facilitate the reduction of Cu^{2+} without favoring the formation of elemental copper (Cu^o), this can be sustained consider the hydrogen spillover phenomena [22]. Hydrogen reduction in silver it is expected to happen at lower temperatures (< 150°C) than in copper, then once reduced, the metallic silver could help into copper reduction by means of the spillover effect. The sample $AgCu_3CLI_45_0$ exhibits close the same behavior described for $CuCLI_45_0$. The fact that there are only changes in amplitude and not in phase

for $AgCu_3CLI_45_0$, is an evidence of the absence of alloy formation. It should be highlight that Ag:Cu alloy is not thermodynamically allowed for bulk system [23]. Finally, the $AgCu_9CLI$ sample exhibits the same behavior as that described for the $AgCu_3CLI$ sample as function of both reduction temperatures (Fib. 1c).

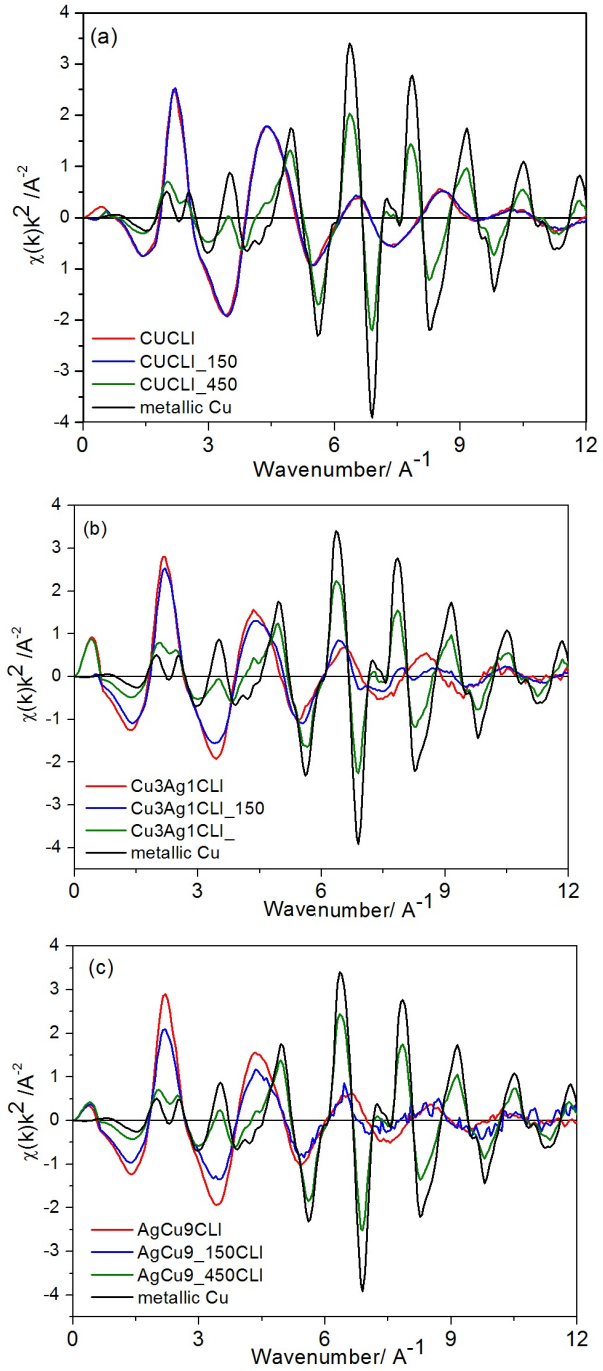

Figure 1. a) Average $\chi(k)\cdot k^2$ data calculated from the Cu–K absorption edge for natural clinoptilolite exchanged only with Cu^{2+} and as function of the reduction temperature. 1b) Average $\chi(k)\cdot k^2$ data calculated from the Cu–K absorption edge for $AgCu_3CLI$ at room temperature and as function of the reduction temperature. c) Average $\chi(k)\cdot k^2$ data calculated from the Cu–K absorption edge for $AgCu_9CLI$ at room temperature and as function of the reduction temperature. In all cases a Cu metal signal is included as a reference signal.

It seems that the volume ratio of dissolved $Cu(NO_3)_2$–$AgNO_3$ used for preparing the bimetallic samples does not influence Cu distances to its nearest neighbors significantly once reduced at the two temperatures. Furthermore the Ag incorporation favors the copper reduction at lower temperatures, and appears to be an efficient tool for the control of the dispersion of the resultant reduced Cu nanoparticles diminishing their size as compared with the sample without silver as will be shown by EXAFS analysis.

Figure 2 shows the magnitude of the Fourier Transform (FT) of the EXAFS signals (k^2 weighted data) of the studied samples as prepared (Cu^{2+} clinoptilolite and Ag–Cu binary mixtures) and the fits for the first shell of oxygen neighbors. This Figure shows also the FT of the EXAFS signal of the CuO standard sample at the top together with its fit assuming the first shell of oxygen neighbors as well. The fit model was based on simple oxygen in tetrahedral coordination for Cu as is in CuO [23].

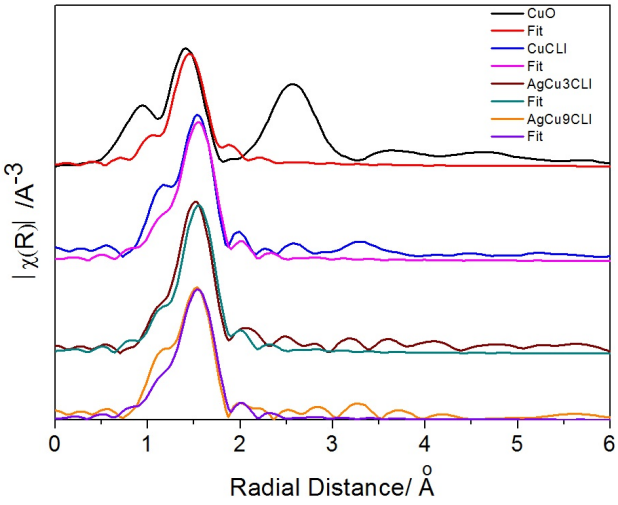

Figure 2. Magnitude of the Fourier Transform (FT) of the EXAFS signals (k^2 weighted data) of the Cu^{2+} clinoptilolite, Ag^+–Cu^{2+} binary mixtures and the CuO reference at room temperature, and fittings with the first shell of O.

Figures 3 and 4 show the FT of the EXAFS signals of the reduced samples at 150°C and 450°C respectively, the last one with fits for the metallic contributions. In each case the FT of the reference Cu metallic sample was included. From these fits and establishing a reasonable hypothesis of the geometrical shape for the nanoparticles is possible determine the size [20]. For a cuboctahedral shape is possible to affirm that CuCLI has a diameter of 1.2 nm, and $AgCu_3CLI$, $AgCu_9CLI$ has 1 nm and 1.4 nm respectively. These estimative can have an error around 20 percent.

Attending to the results shown in Figures 2-4, the samples, CuCLI, $AgCu_3CLI$, $AgCu_9CLI$ and $CuCLI_15_0$, exhibit a typical short-range order behavior. For these samples a single peak at 1.98 å is observed on the fits and it is related with the first coordination sphere of oxygen tetrahedral used as reference. It should be associated with the coordination of Cu^{2+} within the zeolites channels with 4 oxygen atoms of the framework, excluding the possibility of clustering or particle formation. It is in agreement with previous UV-Vis results

reported in [14].

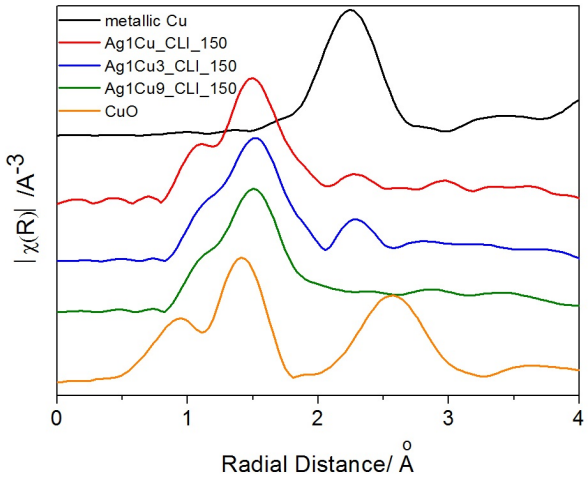

Figure 3. Fourier Transform (FT) of the EXAFS signal for metallic Cu (at the top) and for exchanged natural clinoptilolite samples reduced at 150°C. At the bottom is possible to see the EXAFS signal for a CuO reference.

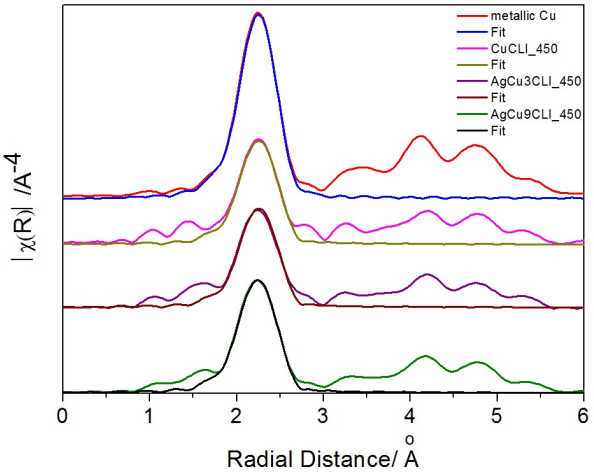

Figure 4. Fourier Transform (FT) and fits for the first shell of EXAFS signals (k^3 weighted data) for metallic Cu and exchanged natural clinoptilolite samples reduced at 450°C

A detailed analysis of the graphs reveals that for the $AgCu_3CLI_15_0$ and $AgCu_9CLI_15_0$ samples, additionally to the principal peak at 1.98 å, a small peak around 2.54 å occurs (obtained by the fit, in graph there is not phase corrected), while for the sample $CuCLI_15_0$ it does not appear. Moreover, with increasing reduction temperature the peak at 1.98 å reduces its amplitude, while for the $CuCLI_45_0$, $AgCu_3CLI_45_0$ and $AgCu_9CLI_45_0$ samples a second peak, at 2.54 å, increases its amplitude reaching its maximum values (Fig. 4). As can be observed from the graphs, the emerging peak as function of temperature must be associated to the first coordination sphere of the metallic copper foil used as reference. The described behavior supports the suggestion made before that the presence of Ag+ may facilitate the reduction of Cu^{2+} . As previously state, the FT of the sample $AgCu_9CLI$ shows the same trend as that described for $AgCu_3CLI$ as function of the temperature.

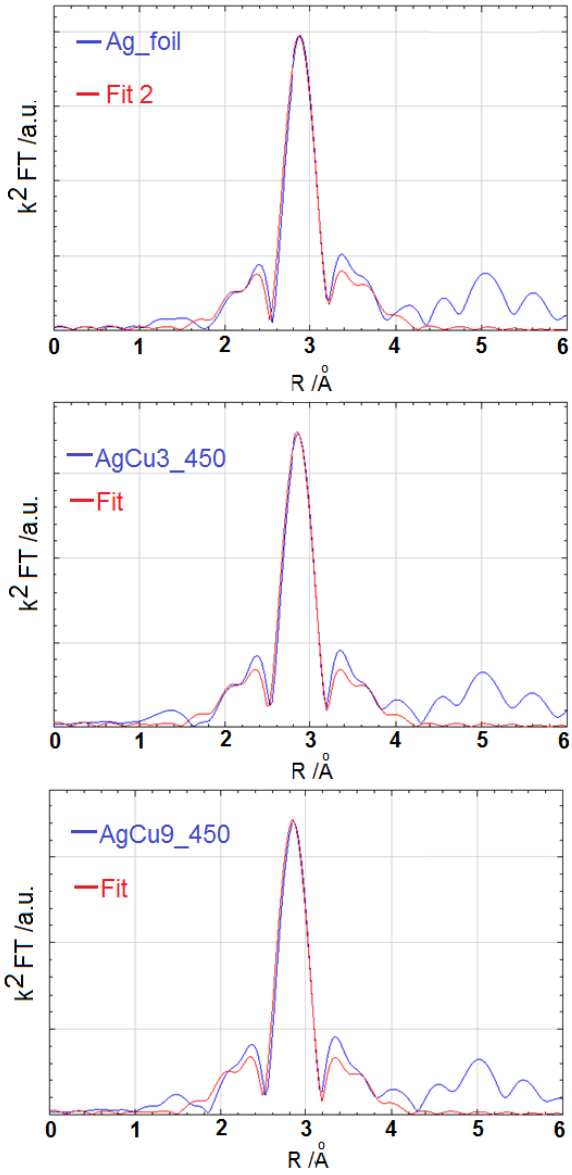

Figure 5. Fourier Transforms (FT) of EXAFS signals (at Ag−K absorption edge) for exchanged natural clinoptilolite samples reduced at 450°C and for the Ag foil used as reference (curves in blue). Fitting of the FTs based on the crystal structure of metallic Ag (fitted curve in red).

The distances associated with the second peak may be related with clustering of Cu−Cu, as commented earlier Cu-Ag particles formation are discarded, for be not compatible with the EXAFS signal in copper edge and not allowed in bulk for thermodinamical reasons [24].

The hypotheses for Cu−Ag nanoalloy formation can be excluded also taking into account the Fourier Transforms (FT) of EXAFS signals (from the Ag-K absorption edge) for exchanged natural clinoptilolite samples reduced at 450°C (Fig. 5). In this figure the FT of the Ag foil used as reference is also included. With increasing reduction temperature silver oxide become metallic Ag given reinforcement to the exclusion of Cu-Ag nanoalloy formation. The estimation for size in the Ag nanoparticles is the following: 2.5 nm for $AgCu_9$ CLI and 3 nm for $AgCu_3$ CLI.

For the reduction temperature of 450°C, most of the Cu and Ag appear as metallic species for exchanged samples, probably outside the zeolite channels. Moreover, the resolved peaks in the FT observed at large distances (long range order) in Fig. 4 and Fig. 5 are related to the subsequent coordination spheres of metallic copper and silver respectively. The former suggests the occurrence of both Cu and Ag nanoparticles.

On the other hand, the little peak still observed for both samples in the phase corrected distance of 1.98 at 450°C corresponds to remaining unreduced Cu^{2+} cations (Fig. 5), but it is not the case for Ag, where the reduction seems to be fully completed.

III.2. HR-XRD EXPERIMENTS

Figure 6 shows the X-ray diffraction patterns (XRD) of CuCLI (bottom of the figure) as well as of $AgCu_9CLI$ before and after reduction at 150°C and 450°C, i.e. $AgCu_9CLI_15_0$ and $AgCu_9CLI_45_0$, respectively. As stated before, the $AgCu_3CLI$ behaves as the $AgCu_9CLI$ one. The qualitative phase analysis of all diffraction patterns confirm that they preserve the C2/*m* and C *mcm* space groups of the main phases of the samples, clinoptilolite and mordenite respectively, after ion exchange. For clarity, only the characteristic maximum for the mordenite phase has been labelled with the Miller index (110)M, while only the maxima (020)C and (200)C have been chosen for representing the clinoptilolite phase.

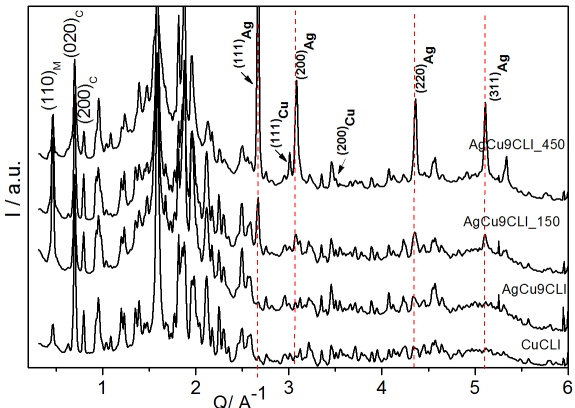

Figure 6. HR-XRDpatterns of the exchanged CuCLI and $AgCu_9CLI$ samples as well as the reduced $AgCu_9CLI_15_0$ and $AgCu_9CLI_45_0$ bimetallic.

For the Ag^+–Cu^{2+} binary sample reduced at 150°C, low intensity peaks corresponding to metallic silver are well observed (dashed vertical lines), while diffraction peaks of metallic copper are absent. It indicates that at 150°C long range order is still missing for Cu, but clustering of Cu–Cu particles with distances close to the first coordination sphere of the metallic Cu (short range order) is possible to sustain as shown in Figure 3.

At 450°C the metal silver (Ag) phase exhibits high and sharp intensity peaks, which in turn indicates that most of the silver appears as metallic Ag with a larger volume fraction in the sample. It is also supported by the results shown in Figure 5. On the other hand, low intensity peaks corresponding to metallic copper start to emerge at this reduction temperature. No alloying of the metallic species is observed. Additionally, the occurrence of well-defined peaks of the Ag – phase already at 150°C and the absence of Cu diffraction peaks allows neglecting the hypotheses previously made about the occurrence of Cu–Ag clusters. It was also confirmed by EXAFS analysis. Then only Cu–Cu clustering can be assumed as responsible for the changes observed in the EXAFS signals (Fig. 1) and in the FTs of the thermal treated $AgCu_3CLI$ and $AgCu_9CLI$ samples respect to the unreduced one (Fig. 2 – 4).

Table 2. Estimated FWHM values for (111)Cu and (200)Ag reflections.

sample	FWHM for (111)Cu	FWHM for (200)Ag
$CuCLI_45_0$	(0.173 ± 0.002)°	-
$AgCu_9CLI_45_0$	(0.179± 0.002)°	(0.301± 0.002)°

Another important feature of the HR-XRD patterns is presented in the Figure 7, where the peaks of metallic Cu and Ag in the range 2.5 – 5.2 å$^{-1}$ for $CuCLI_45_0$ and $AgCu_9CLI_45_0$ samples appear. Comparing the relative intensity of the Cu reflections for both samples it seems that agglomeration of reduced copper is inhibit in presence of silver as shown in the EXAFS results.

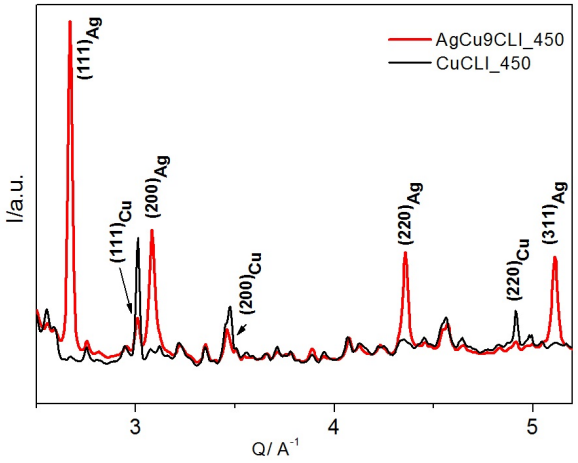

Figure 7. HR-XRD patterns in the range 2.5 – 5.2 å$^{-1}$ for the $CuCLI_45_0$ and $AgCu_9CLI_45_0$ samples.

Particle size determination from the diffraction profiles was not possible because the large degree of overlapping of peaks of different phases. However, an attempt for a qualitative analysis taking into account the Full Width at Half Maximum (FWHM) of the (111)Cu and (200)Ag peaks was made. Table 2 shows the estimated FWHM values for each reflection. The FWHM value for the reflection (111)Cu in both samples is unchanged, which in turn means no change in Cu particle size at this reduction temperature even in presence of Ag. On the other hand, Ag particles size seems to be smaller than Cu one.

IV. CONCLUSIONS

The EXAFS signals of both bimetallic samples show important changes of period and amplitude after their reduction at 150°C, indicating that Cu^{2+} coordination is

affected and that reduction of this cation occurs. It does not happen to Cu monometallic system one. Thus, the presence of silver promotes the Cu^{2+} reduction in Cu−Ag bimetallic systems that can be explained by the spillover phenomena. According to XRD and EXAFS results, only silver clusters are formed in both bimetallic samples reduced at 150°C. At higher reduction temperature (450°C) most of copper and silver appear as elemental metallic species for all samples, probably outside the zeolite channels. The study revealed that agglomeration of reduced copper is limited in presence of silver.

The metallic silver species formed during the reduction process drive the reduction of copper oxides in the ionic exchanged structure and finally drives the agglomeration of the reduced neutral copper atoms through small clusters at the surface, at lower temperatures of around 150°C, this process increases until higher size particles at higher temperature of 150°C occur.

ACKNOWLEDGEMENTS

EXAFS experiments have been supported by the Brazilian Synchrotron Light Laboratory (LNLS) under proposal D04B - XAFS1 7770. ICTP - Elettra Synchrotron, Trieste, Italy is also knowledge for financial support in the framework of the proposal: 20110280.

Authors thank the support from grants UNAM-PAPIIT-IN107817 and SENER-CONACYT-Hydrocarbons No 117373 (Mexico), and the project 18-53-34004 Russia-Cuba (RFBR-CITMA).This work was also supported in the framework of a scientific project associated to the national program of fundamental science (MES–UH-2018). F. Chavez-Rivas acknowledges support from COFAA-IPN-México.

REFERENCIAS

[1] R.E. Ramírez-Garza, I. Rodríguez-Iznaga, A. Simakov, M.H. Farías, F.F. Castillón-Barraza, Mater. Res. Bull. **97** 369, (2018).

[2] G. Yao, J. Lei, W. Zhang, C. Yu, Z. Sun, S. Zheng, S. Komarneni, Environ. Sci. Pollut. Res. **26**, 262782 (2019).

[3] L. Bacakova, M. Vandrovcova, I. Kopova, I. Jirka, Biomater. Sci., 6974 (2018).

[4] I. Rodríguez-Iznaga, V. Petranovskii, G. Rodríguez-Fuentes, C. Mendoza, A. Benitez-Aguilar, J. Colloid Interface Sci **316**, 877 (2007).

[5] B. Concepción-Rosabal, G. Rodríguez-Fuentes, N. Bogdanchikova, P. Bosch, M. Avalos, and V.H. Lara, Microporous Mesoporous Mater. **86**, 249 (2005).

[6] S.Y. Joshi, A. Kumar, J. Luo, K. Kamasamudram, N.W. Currier and A.Yezerets, Appl. Catal. B **226**, 565 (2018).

[7] J.F. Gelves, L. Dorkis, M.A. Márquez, A.C. Álvarez, L.M. González and A.L. Villa, Catal. Today **320**, 112 (2019).

[8] J. Vergara-Figueroa, S. Alejandro-Martín, H. Pesenti, F. Cerda, A. Fernández-Pérez and W. Gacitúa, Materials **12**, 2202 (2019).

[9] S. Chaturvedi and P. N. Dave, Chem. Methodol. **3**, 115 (2019).

[10] J.M. Fedeyko, H. Chen, T.H. Ballinger, E.C. Weigert, H. Chang, J.P. Cox, P.J. Andersen, SAE Technical Paper 2009-01-0899, (2009), https://doi.org/10.4271/2009-01-0899.

[11] M. Jablonska, R. Palkovits, Appl. Catal. B. **181**, 332 (2016).

[12] L. Zhang, Q. Wu, X. Meng, U. Müller, M. Feyen, D. Dai, S. Maurer, R. McGuire, A. Moini et. al., React. Chem. Eng. **4**, 975 (2019).

[13] Y. Shan, X. Shi, J. Du, Y. Yu and H. He, Catal. Sci. Technol. **9**, 106 (2019).

[14] I. Rodríguez-Iznaga, V. Petranovskii, F. Castillón-Barraza and B. Concepción-Rosabal, J. Nanosci. Nanotechnol. **11**, 1 (2011).

[15] I. Rodríguez-Iznaga, V. Petranovskii, F.F. Castillón and M.H. Farias, Opt. Mater. **29**, 105 (2006).

[16] P. Sánchez-López, Y. Kotolevich, S. Miridonov, F. Chávez-Rivas, S. Fuentes, and V. Petranovskii, Catalysts **9**, 58 (2019).

[17] M. Chen, Q. Sun, X. Yang, and J. Yu, Inorg. Chem. Commun. **105**, 203 (2019).

[18] B. Concepción-Rosabal, A. Pentón-Madrigal, E. Estévez-Rams, N. Bogdanchikova, M. Avalos-Borja. Rev. Cubana Fis. **25**, 136 (2008).

[19] S.J.A. Figueroa, J.C. Mauricio, J. Murari, D.B. Beniz, J.R. Piton, H.H. Slepicka, M. Falcao de Sousa, A.M. Espindola, and A.P.S. Levinsky, J. Phys.: Conf. Ser. **712**, 012022 (2016).

[20] B. Ravel and M. Newville, J. Synch. Rad. **12**, 537 (2005).

[21] A. M. Beale and B. M. Weckhuysen, Phys. Chem. Chem. Phys. **12**, 5562 (2010).

[22] R. Prins, Chem. Rev. 112, 2714 (2012).

[23] Inorganic Crystal Structure Database (ICSD), Version: 2008-1. https://icsd.products.fiz-karlsruhe.de/.

[24] G. Bergerhoff, I.D. Brown in "Crystallographic Databases", F.H. Allen et al. (Hrsg.) Chester, International Union of Crystallography, (1987).